中国科学院理论物理研究所
Institute of Theoretical Physics, Chinese Academy of Sciences

普朗克卫星2015年的宇宙学结果

郭宗宽

中国科技大学交叉学科理论研究中心

2015.4.7

CMB的产生和发现

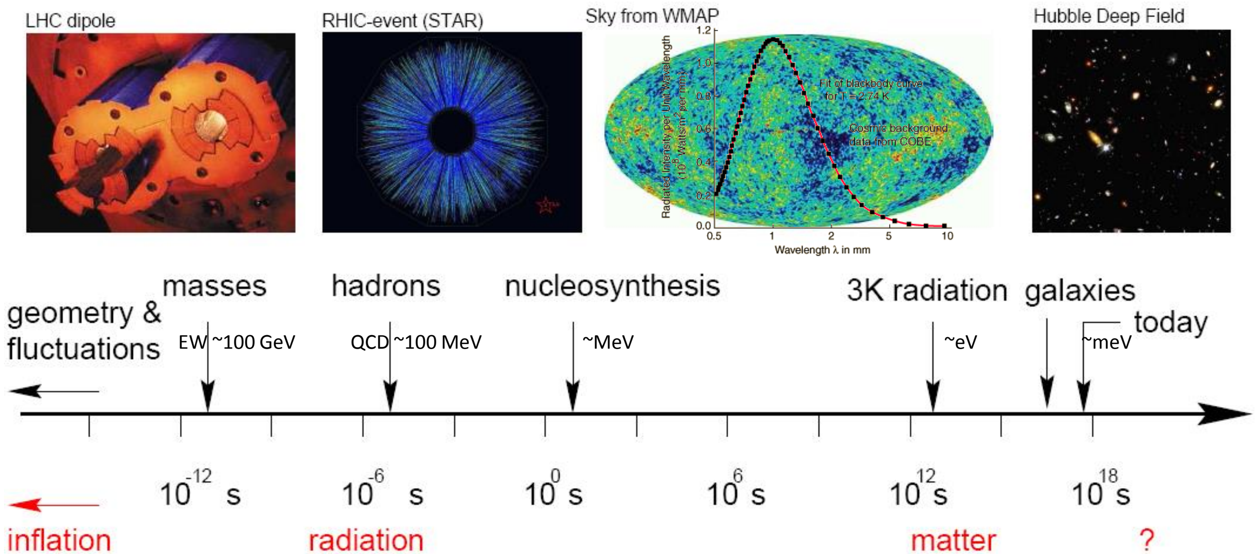

$$p + e^- \leftrightarrow H + \gamma$$

$$\gamma + e^- \leftrightarrow \gamma + e^-$$

decoupling during ***recombination***

$400\ \mathrm{cm}^{-3}$ now

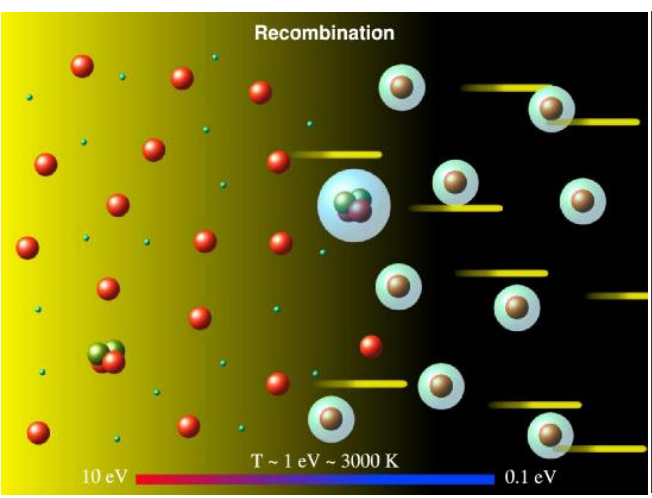

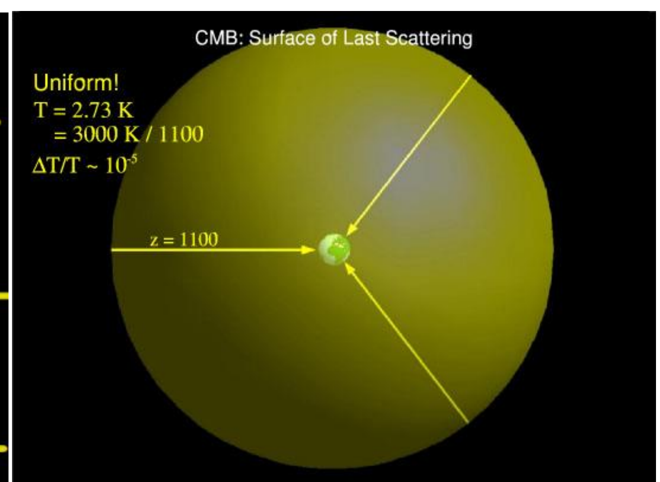

Predicted by Gamow et al in 1948,
Discovered by Penzias and Wilson in 1964-1965, 1978
Interpreted by Peebles et al in 1965

CMB各向异性的物理起源

$$\delta\phi \Leftrightarrow \delta g_{\mu\nu} \Leftrightarrow \delta f \Leftrightarrow \delta T, U, Q \rightarrow C_l$$

$$\frac{\Delta T(\hat{n})}{T} = \sum_{lm} a_{lm} Y_{lm}(\hat{n})$$

$$a_{lm} = \int d\hat{n}\, Y^*_{lm}(\hat{n}) \frac{\Delta T(\hat{n})}{T}$$

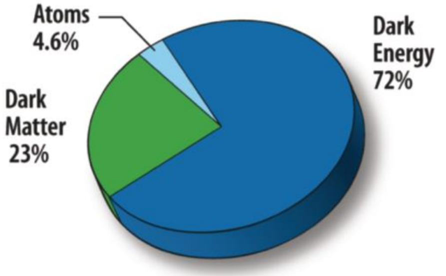

Today

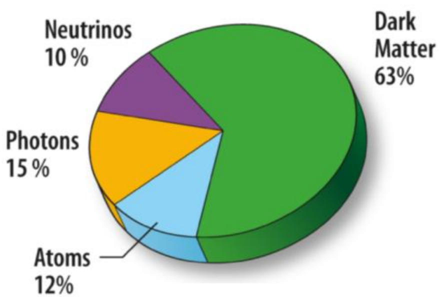

CMB ERA

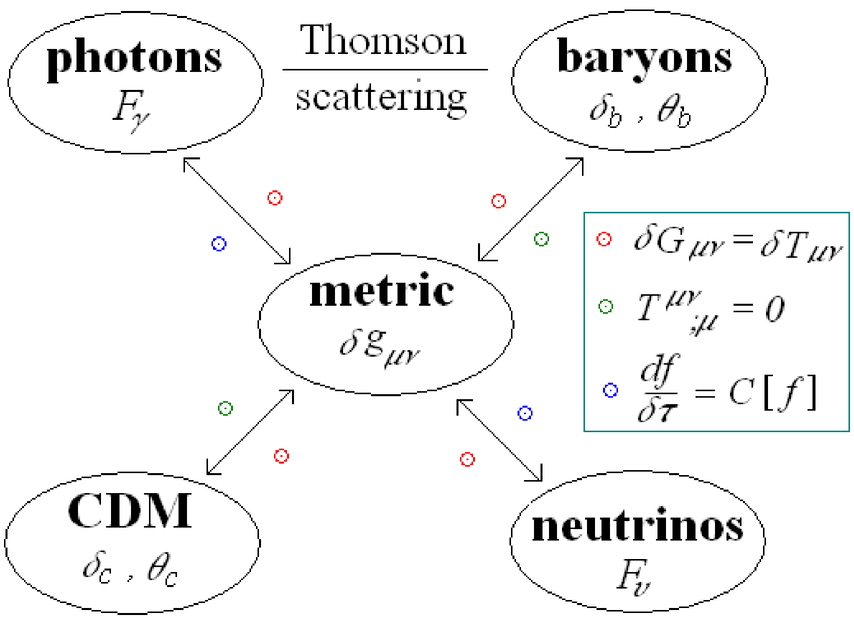

CMB各向异性的探测

1. Ground-based experiments
2. Balloon-borne experiments
3. Space experiments

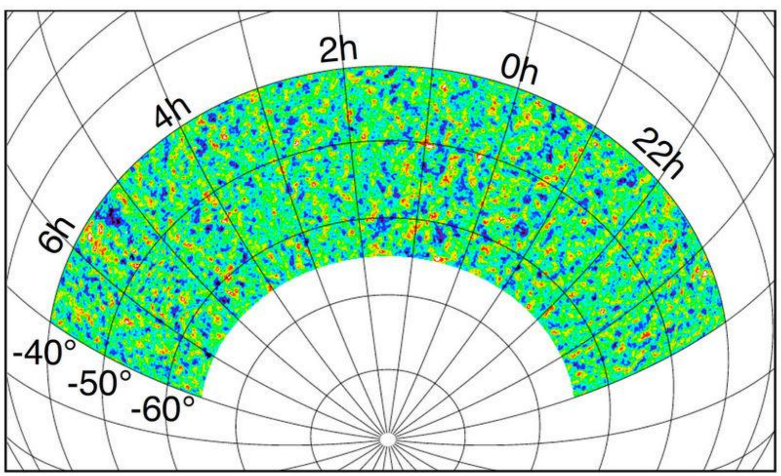

SPT 2008-2011

VS

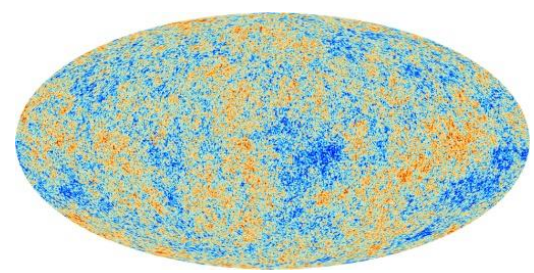

Planck 2013

名称	地点	时间	状态	*l* 范围	频率 (GHz)	极化
ACBAR	南极	2001~2008	完成	60~2700	150,219,274	无
CBI	智利	2002~2008	完成	300~3000	26~36	无
VSA	西班牙	2002~2004	完成	130~1800	26~36	无
SPT	南极	2007~	进行中	650~9500	95,150,220	无
ACT	智利	2008~	进行中	500~10000	148,218,277	无
DASI	南极	2001~2003	完成	200~900	26~36	有
CAPMAP	美国	2002~2008	完成	500~1500	40,100	有
QUaD	南极	2005~2010	完成	200~2000	100,150	有
BICEP	南极	2006~2008	完成	21~335	100,150,220	有
QUIET	智利	2008~2010	完成	60~3500	40,90	有
BICEP2	南极	2009~2012	完成	21~335	150	有
KECKArray	南极	2010~	进行中	21~335	150	有
ABS	智利	2011~	进行中	25~200	145	有
POLARBEAR	智利	2012~	进行中	50~2000	90,150	有
SPTpol	南极	2012~	进行中	501~5000	95,150	有
ACTpol	智利	2013~	进行中	225~8725	90,146	有
BICEP3	南极	2016~	计划中	--	95	有
CLASS	智利	--	计划中	--	40, 90, 150,220	有

气球探测实验

名称	地点	时间	状态	*l* 范围	频率 (GHz)	极化
MAXIMA	美国	1995,98,99	完成	50~700	150~420	无
BOOMERanG	南极	1997~2003	完成	25~1025	90~420	有
EBEX	南极	2012~	进行中	25~1000	150,250,410	有
SPIDER	南极	2013,2015	进行中	10~300	90,150,280	有
PIPER	--	2015~	计划中	--	200,270,350,600	有

空间探测实验

名称	卫星发射	时间	状态	l 范围	频率 (GHz)	极化
COBE	NASA	1989~1993	完成	2~40	31.5, 53, 90	无
WMAP	NASA	2001~2010	完成	2~1200	23, 33, 41, 61, 94	有
Planck	ESA	2009~	进行中	2~2500	30,44,70,100~857	有
CMBPol	NASA	--	计划中	--	--	有
COrE	ESA	--	计划中	--	--	有

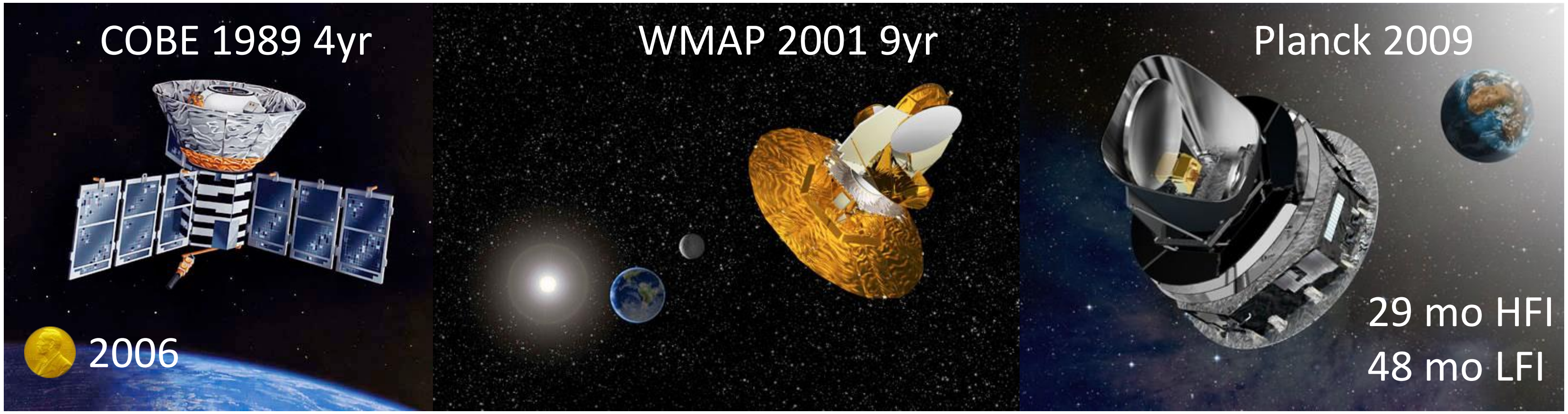

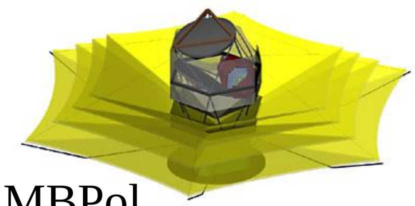
NASA: CMBPol


ESA: COrE

粒子物理	宇宙学
19参数的标准模型	6参数的标准模型
超标准模型，新物理	超标准模型，新物理
弱简并	强简并
LHC（$80亿）	普朗克卫星（€7亿）
TeV	近普朗克能标

We know much but understand little.

http://www.cosmos.esa.int/web/planck/home

SRE SCIENCE MISSIONS | SCIENCE & TECHNOLOGY | EUROPEAN SPACE AGENCY | SIGN IN

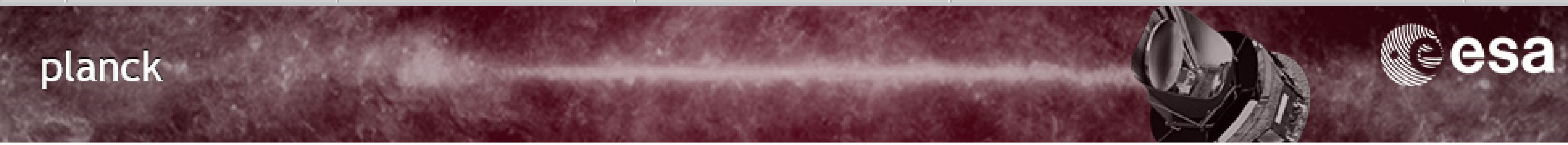

Cosmos » Planck » Home

- Home
- Mission Overview
- Mission History
- Planck Legacy Archive
- Publications
- Picture Gallery
- Conferences
- Planck Teams
- Restricted Planck Items

PLANCK SCIENCE TEAM HOME

The 2015 release to the public of Planck data and scientific results is staged as follows:

- The data products and scientific results have been presented in December 2014 at public conferences in Ferrara and Paris. Most presentations made in Ferrara are available here. Videos of presentations in Paris are available here.

- The 2015 release to the public of full mission data products and scientific papers has taken place on 5 February at 15:00 CET. The data are available via the Planck Legacy Archive. Scientific papers are available here.

- Additional 2015 products will be released near the end of March 2015.

Go directly to Planck

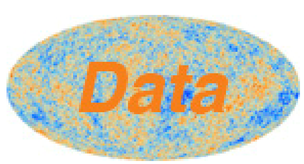

PLANCK STATUS

Mission status: Planck stopped operations on 23 October 2013.

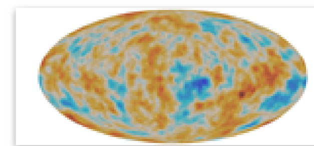

LATEST NEWS

- **Results of a joint analysis of BICEP2/Keck and Planck data:** a joint analysis of data from ESA's Planck satellite and the ground-based BICEP2 and Keck Array experiments has found no conclusive evidence of primordial gravitational waves. Read the story. Download the paper.
- **The magnetic field structure in the Rosette**

普朗克卫星2013年的结果

I. Overview of products and results
II. Low Frequency Instrument data processing
III. LFI systematic uncertainties
IV. LFI beams and window functions
V. LFI calibration
VI. High Frequency Instrument data processing
VII. HFI time response and beams
VIII. HFI photometric calibration and mapmaking
IX. HFI spectral response
X. HFI energetic particle effects: characterization, removal, and simulation
XI. All-sky model of thermal dust emission
XII. Diffuse component separation
XIII. Galactic CO emission
XIV. Zodiacal emission

XV. CMB power spectra and likelihood

XVI. Cosmological parameters (Cited by 3284 records, i.e., very active)

XVII. Gravitational lensing by large-scale structure

XVIII. The gravitational lensing-infrared background correlation

XIX. The integrated Sachs-Wolfe effect

XX. Cosmology from Sunyaev-Zeldovich cluster counts

XXI. Power spectrum and high-order statistics of the Planck all-sky Compton parameter map

XXII. Constraints on inflation

XXIII. Isotropy and statistics of the CMB

XXIV. Constraints on primordial non-Gaussianity

XXV. Searches for cosmic strings and other topological defects

XXVI. Background geometry and topology of the Universe

XXVII. Doppler boosting of the CMB: Eppur si muove

XXVIII. The Planck Catalogue of Compact Sources

XXIX. The Planck catalogue of Sunyaev-Zeldovich sources

XXX. Cosmic infrared background measurements and implications for star formation

XXXI. Consistency of the Planck data

普朗克卫星2015年的结果

I. Overview of products and results

II. Low Frequency Instrument data processing

III. LFI systematic uncertainties

IV. LFI beams and window functions

V. LFI calibration

VI. LFI maps

VII. High Frequency Instrument data processing: Time-ordered information and beam processing

VIII. HFI data processing: Calibration and maps

IX. Diffuse component separation: CMB maps

X. Diffuse component separation: Foreground maps

XI. CMB power spectra, likelihood, and consistency of cosmological parameters

XII. Simulations

XIII. Cosmological parameters (Cited by 108 records)

XIV. Dark energy and modified gravity

XV. Gravitational lensing

XVI. Isotropy and statistics of the CMB

XVII. Primordial non-Gaussianity

XVIII. Background geometry and topology of the Universe

XIX. Constraints on primordial magnetic fields

XX. Constraints on inflation

XXI. The integrated Sachs-Wolfe effect

XXII. A map of the thermal Sunyaev-Zeldovich effect

XXIII. Thermal Sunyaev-Zeldovich effect–cosmic infrared background correlation

XXIV. Cosmology from Sunyaev-Zeldovich cluster counts

XXV. Diffuse, low-frequency Galactic foregrounds

XXVI. The Second Planck Catalogue of Compact Sources

XXVII. The Second Planck Catalogue of Sunyaev-Zeldovich Sources

XXVIII. The Planck Catalogue of Galactic Cold Clumps

Planck 2013 vs. 2015

	Planck 2013	*Planck 2015*
Data	15.5 months	29 months for HFI 48 months for LFI
Systematic	4K cooler lines; calibration offset; beam; deglitching algorithm; *et al*.	
Spectra	TT	TT, TE, EE
Large-scale	+WP ($2<l<49$)	+lowP ($2<l<29$)
Likelihood	CamSpec (50~2500)	Plik (30~2500)
Parameters	n_s, H_0, τ	

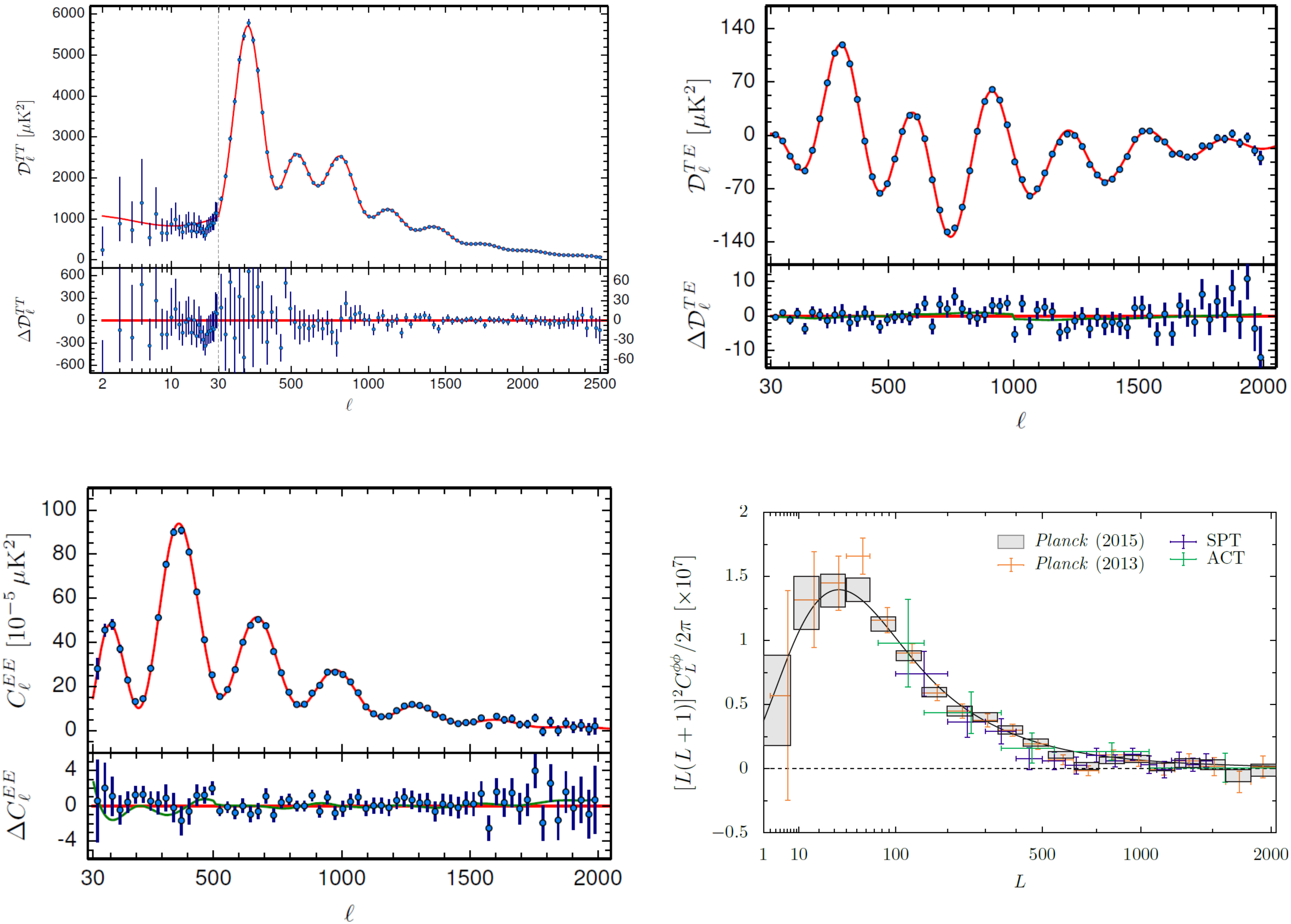

$\mathcal{D}_\ell^{TT}$ [μK^2]
6000
5000
4000
3000
2000
1000
0
$\Delta\mathcal{D}_\ell^{TT}$
600
300
0
-300
-600
60
30
0
-30
-60
2
10
30
500
1000
1500
2000
2500
ℓ
$\mathcal{D}_\ell^{TE}$ [μK^2]
140
70
0
-70
-140
$\Delta\mathcal{D}_\ell^{TE}$
10
0
-10
30
500
1000
1500
2000
ℓ
C_ℓ^{EE} [$10^{-5}\,\mu$K^2]
100
80
60
40
20
0
ΔC_ℓ^{EE}
4
0
-4
30
500
1000
1500
2000
ℓ
$[L(L+1)]^2 C_L^{\phi\phi}/2\pi$ [$\times 10^7$]
2
1.5
1
0.5
0
−0.5
Planck (2015)
Planck (2013)
SPT
ACT
1
10
100
500
1000
2000
L

Planck2015之后的标准宇宙学手册

Parameter	TT+lowP 68 % limits	TT+lowP+lensing 68 % limits	TT+lowP+lensing+ext 68 % limits	TT,TE,EE+lowP 68 % limits	TT,TE,EE+lowP+lensing 68 % limits	TT,TE,EE+lowP+lensing+ext 68 % limits
$\Omega_b h^2$	0.02222 ± 0.00023	0.02226 ± 0.00023	0.02227 ± 0.00020	0.02225 ± 0.00016	0.02226 ± 0.00016	0.02230 ± 0.00014
$\Omega_c h^2$	0.1197 ± 0.0022	0.1186 ± 0.0020	0.1184 ± 0.0012	0.1198 ± 0.0015	0.1193 ± 0.0014	0.1188 ± 0.0010
$100\theta_{MC}$	1.04085 ± 0.00047	1.04103 ± 0.00046	1.04106 ± 0.00041	1.04077 ± 0.00032	1.04087 ± 0.00032	1.04093 ± 0.00030
τ	0.078 ± 0.019	0.066 ± 0.016	0.067 ± 0.013	0.079 ± 0.017	0.063 ± 0.014	0.066 ± 0.012
$\ln(10^{10} A_s)$	3.089 ± 0.036	3.062 ± 0.029	3.064 ± 0.024	3.094 ± 0.034	3.059 ± 0.025	3.064 ± 0.023
n_s	0.9655 ± 0.0062	0.9677 ± 0.0060	0.9681 ± 0.0044	0.9645 ± 0.0049	0.9653 ± 0.0048	0.9667 ± 0.0040
H_0	67.31 ± 0.96	67.81 ± 0.92	67.90 ± 0.55	67.27 ± 0.66	67.51 ± 0.64	67.74 ± 0.46
Ω_Λ	0.685 ± 0.013	0.692 ± 0.012	0.6935 ± 0.0072	0.6844 ± 0.0091	0.6879 ± 0.0087	0.6911 ± 0.0062
Ω_m	0.315 ± 0.013	0.308 ± 0.012	0.3065 ± 0.0072	0.3156 ± 0.0091	0.3121 ± 0.0087	0.3089 ± 0.0062
$\Omega_m h^2$	0.1426 ± 0.0020	0.1415 ± 0.0019	0.1413 ± 0.0011	0.1427 ± 0.0014	0.1422 ± 0.0013	0.14170 ± 0.00097
$\Omega_m h^3$	0.09597 ± 0.00045	0.09591 ± 0.00045	0.09593 ± 0.00045	0.09601 ± 0.00029	0.09596 ± 0.00030	0.09598 ± 0.00029
σ_8	0.829 ± 0.014	0.8149 ± 0.0093	0.8154 ± 0.0090	0.831 ± 0.013	0.8150 ± 0.0087	0.8159 ± 0.0086
$\sigma_8 \Omega_m^{0.5}$	0.466 ± 0.013	0.4521 ± 0.0088	0.4514 ± 0.0066	0.4668 ± 0.0098	0.4553 ± 0.0068	0.4535 ± 0.0059
$\sigma_8 \Omega_m^{0.25}$	0.621 ± 0.013	0.6069 ± 0.0076	0.6066 ± 0.0070	0.623 ± 0.011	0.6091 ± 0.0067	0.6083 ± 0.0066
z_{re}	$9.9^{+1.8}_{-1.6}$	$8.8^{+1.7}_{-1.4}$	$8.9^{+1.3}_{-1.2}$	$10.0^{+1.7}_{-1.5}$	$8.5^{+1.4}_{-1.2}$	$8.8^{+1.2}_{-1.1}$
$10^9 A_s$	$2.198^{+0.076}_{-0.085}$	2.139 ± 0.063	2.143 ± 0.051	2.207 ± 0.074	2.130 ± 0.053	2.142 ± 0.049
$10^9 A_s e^{-2\tau}$	1.880 ± 0.014	1.874 ± 0.013	1.873 ± 0.011	1.882 ± 0.012	1.878 ± 0.011	1.876 ± 0.011
Age/Gyr	13.813 ± 0.038	13.799 ± 0.038	13.796 ± 0.029	13.813 ± 0.026	13.807 ± 0.026	13.799 ± 0.021
z_*	1090.09 ± 0.42	1089.94 ± 0.42	1089.90 ± 0.30	1090.06 ± 0.30	1090.00 ± 0.29	1089.90 ± 0.23
r_*	144.61 ± 0.49	144.89 ± 0.44	144.93 ± 0.30	144.57 ± 0.32	144.71 ± 0.31	144.81 ± 0.24
$100\theta_*$	1.04105 ± 0.00046	1.04122 ± 0.00045	1.04126 ± 0.00041	1.04096 ± 0.00032	1.04106 ± 0.00031	1.04112 ± 0.00029
z_{drag}	1059.57 ± 0.46	1059.57 ± 0.47	1059.60 ± 0.44	1059.65 ± 0.31	1059.62 ± 0.31	1059.68 ± 0.29
r_{drag}	147.33 ± 0.49	147.60 ± 0.43	147.63 ± 0.32	147.27 ± 0.31	147.41 ± 0.30	147.50 ± 0.24
k_D	0.14050 ± 0.00052	0.14024 ± 0.00047	0.14022 ± 0.00042	0.14059 ± 0.00032	0.14044 ± 0.00032	0.14038 ± 0.00029
z_{eq}	3393 ± 49	3365 ± 44	3361 ± 27	3395 ± 33	3382 ± 32	3371 ± 23
k_{eq}	0.01035 ± 0.00015	0.01027 ± 0.00014	0.010258 ± 0.000083	0.01036 ± 0.00010	0.010322 ± 0.000096	0.010288 ± 0.000071
$100\theta_{s,eq}$	0.4502 ± 0.0047	0.4529 ± 0.0044	0.4533 ± 0.0026	0.4499 ± 0.0032	0.4512 ± 0.0031	0.4523 ± 0.0023

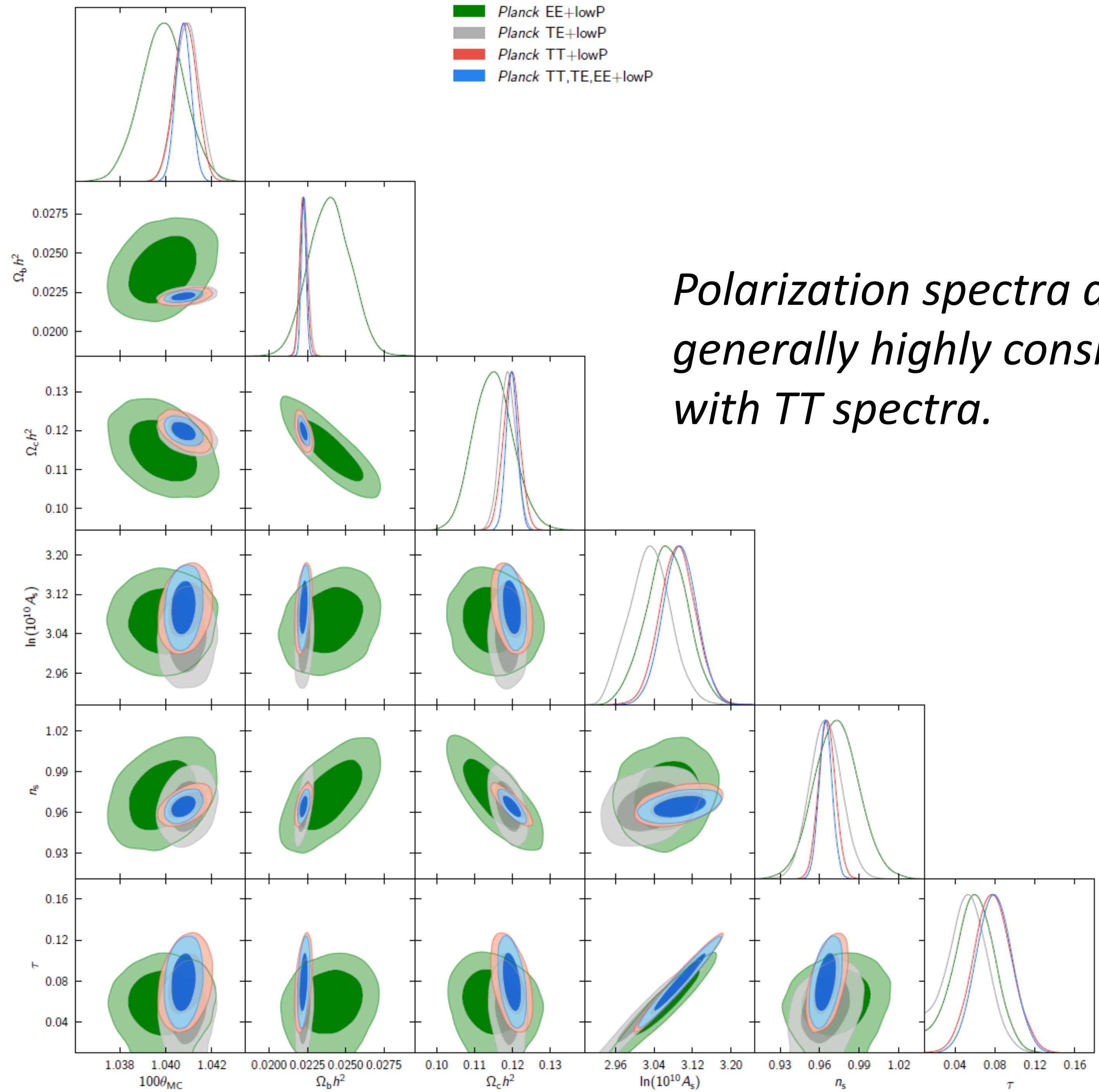

Polarization spectra are generally highly consistent with TT spectra.

Planck 2015 results. XIII. Cosmological parameters

February 5 2015

ABSTRACT

This paper presents cosmological results based on full-mission *Planck* observations of temperature and polarization anisotropies of the cosmic microwave background (CMB) radiation. Our results are in very good agreement with the 2013 analysis of the *Planck* nominal-mission temperature data, but with increased precision. The temperature and polarization power spectra are consistent with the standard spatially-flat six-parameter ΛCDM cosmology with a power-law spectrum of adiabatic scalar perturbations (denoted "base ΛCDM" in this paper). From the *Planck* temperature data combined with *Planck* lensing, for this cosmology we find a Hubble constant, $H_0 = (67.8 \pm 0.9)$ km s^{-1}l sity parameter $\Omega_m = 0.308 \pm 0.012$, and a tilted scalar spectral index with $n_s = 0.968 \pm 0.006$, consistent with the 2013 analysi ve quote 68 % confidence limits on measured parameters and 95 % upper limits on other parameters.) We present the first resu measurements with the Low Frequency Instrument at large angular scales. Combined with the *Planck* temperature and lensing ements give a reionization optical depth of $\tau = 0.066 \pm 0.016$, corresponding to a reionization redshift of $z_{re} = 8.8^{+1.7}_{-1.4}$. These ent with those from WMAP polarization measurements cleaned for dust emission using 353 GHz polarization maps from the astrument. We find no evidence for any departure from base ΛCDM in the neutrino sector of the theory. For example, combining *Planck* observations with other astrophysical data we find $N_{eff} = 3.15 \pm 0.23$ for the effective number of relativistic degrees of freedom, consistent with the value $N_{eff} = 3.046$ of the Standard Model of particle physics. The sum of neutrino masses is constrained to $\sum m_\nu < 0.23$ eV. The spatial curvature of our Universe is found to be very close to zero with $|\Omega_K| < 0.005$. Adding a tensor component as a single-parameter extension to base ΛCDM we find an upper limit on the tensor-to-scalar ratio of $r_{0.002} < 0.11$, consistent with the *Planck* 2013 results and consistent with the *B*-mode polarization constraints from a joint analysis of BICEP2, *Keck Array*, and *Planck* (BKP) data. Adding the BKP *B*-mode data to our analysis leads to a tighter constraint of $r_{0.002} < 0.09$ and disfavours inflationary models with a $V(\phi) \propto \phi^2$ potential. The addition of *Planck* polarization data leads to strong constraints on deviations from a purely adiabatic spectrum of fluctuations. We find no evidence for any contribution from isocurvature perturbations or from cosmic defects. Combining *Planck* data with other astrophysical data, including Type Ia supernovae, the equation of state of dark energy is constrained to $w = -1.006 \pm 0.045$, consistent with the expected value for a cosmological constant. The standard big bang nucleosynthesis predictions for the helium and deuterium abundances for the best-fit *Planck* base ΛCDM cosmology are in excellent agreement with observations. We also analyse constraints on annihilating dark matter and on possible deviations from the standard recombination history. In both cases, we find no evidence for new physics. The *Planck* results for base ΛCDM are in good agreement with baryon acoustic oscillation data and with the JLA sample of Type Ia supernovae. However, as in the 2013 analysis, the amplitude of the fluctuation spectrum is found to be higher than inferred from some analyses of rich cluster counts and weak gravitational lensing. We show that these tensions cannot easily be resolved with simple modifications of the base ΛCDM cosmology. Apart from these tensions, the base ΛCDM cosmology provides an excellent description of the *Planck* CMB observations and many other astrophysical data sets.

01. 标准模型 — 物质密度参数
02. 标准模型 — 哈勃常数
03. 标准模型 — 再电离
04. 标准模型 — 声学尺度
05. 标准模型 — 物质密度扰动
06. 标准模型 — 原初曲率扰动的谱指标
07. 超标准模型 — 暗能量和修改引力
08. 超标准模型 — 原初引力波
09. 超标准模型 — 原初曲率扰动的功率谱性质
10. 超标准模型 — 同曲率扰动
11. 超标准模型 — 原初非高斯
12. 超标准模型 — 空间拓扑
13. 超标准模型 — 中微子物理
14. 超标准模型 — 原初氦合成
15. 超标准模型 — 暗物质湮灭
16. 超标准模型 — 原初磁场

1. 标准模型 — 物质密度参数

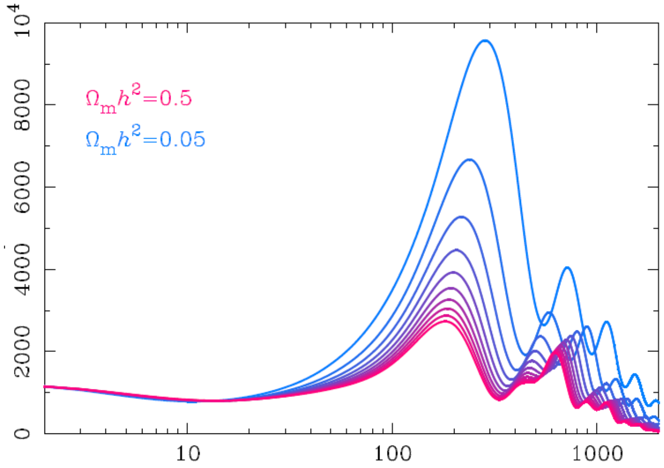

Planck 2013 TT+WP:

$$\Omega_m = 0.315 \pm 0.017$$

Planck 2015 TT+lowP:

$$\Omega_m = 0.315 \pm 0.013$$

***SNLS compilation* (473)**: 123 low-redshifts, 242 3yr-SNLS, 93 SDSS, 14 HST

$$\Omega_m = 0.227$$

a 2σ discrepancy

***JLA sample* (740)**: 118 low-redshifts, 239 3yr-SNLS, 374 SDSS-II, 9 HST

$$\Omega_m = 0.295 \pm 0.034$$

disappear

2. 标准模型 — 哈勃常数

$H_0 = (67.3 \pm 1.2)\ \mathrm{km\ s^{-1} Mpc^{-1}}$ (Planck 2013 TT+WP)

$H_0 = (67.31 \pm 0.96)\ \mathrm{km\ s^{-1} Mpc^{-1}}$ (Planck 2015 TT+lowP)

Riess 2011: Cepheids+8 Sne Ia

$H_0 = (73.8 \pm 2.4)\ \mathrm{km\ s^{-1} Mpc^{-1}}$ a 2.5σ discrepancy

Efstathiou 2014: NGC 4258

$H_0 = (70.6 \pm 3.3)\ \mathrm{km\ s^{-1} Mpc^{-1}}$ disappear

RG Cai, ZK Guo, B Tang, Phys. Rev. D89 (2014) 123518.

3. 标准模型 — 再电离

$\tau = 0.089^{+0.012}_{-0.014}$, $z_{\rm re} = 11.1 \pm 1.1$ (Planck 2013 TT+WP)

Fan 2006: the evolution of the inter-galactic Lyα opacity measured in the spectra of quasars

$z_{\rm re} \approx 6$ significantly low

$\tau = 0.066 \pm 0.016$, $z_{\rm re} = 8.8^{+1.7}_{-1.4}$ (Planck 2015 TT+lowP+lens)

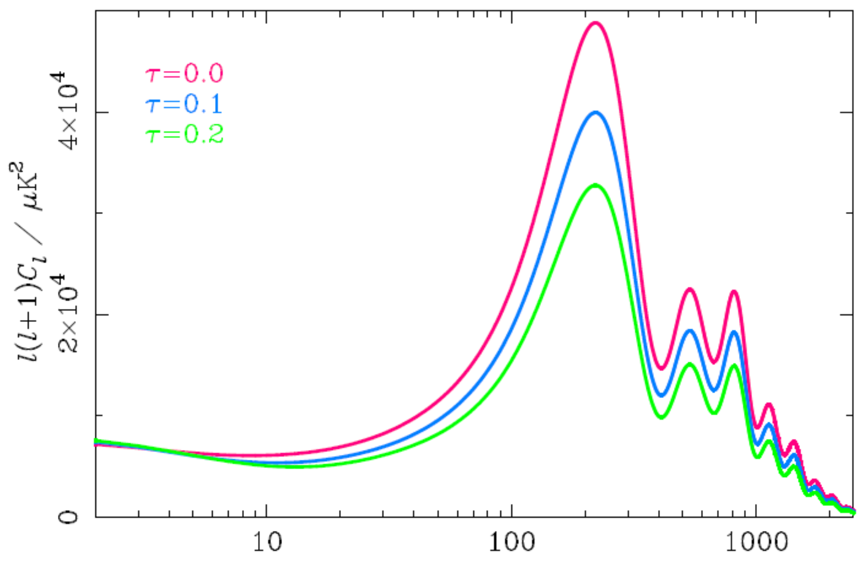

consistent

4. 标准模型 – 声学尺度

BAO measurements:

6dFGS (z=0.1),
SDSS-MGS (z=0.57),
BOSS-LOWZ (z=0.32),
BOSS-CMASS (z=0.57),
WiggleZ (0.44,0.60,0.73)

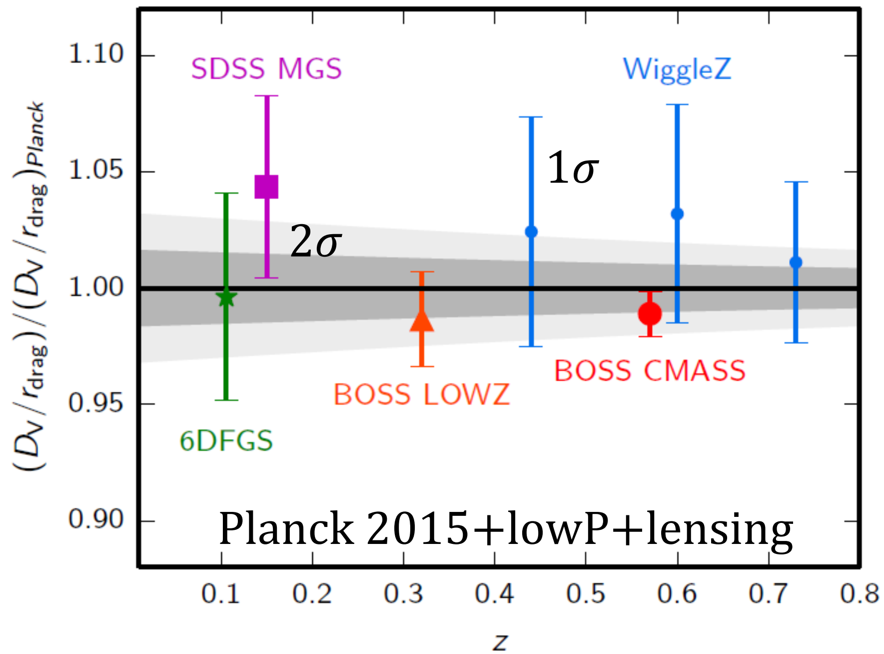

Lyα BAO measurements: the Lyα forest with quasars

$$\frac{c}{H(2.34)r_{\rm drag}} = 9.14 \pm 0.20 \text{ (Lyα BAO)}$$

a 2.7σ discrepancy

$$\frac{c}{H(2.34)r_{\rm drag}} = 8.586 \pm 0.021 \text{ (Planck 2015 TT+lowP+lens)}$$

5. 标准模型 — 物质密度扰动

$\sigma_8 = 0.829 \pm 0.012$ (Planck 2013 TT+WP)

$\sigma_8 = 0.829 \pm 0.014$ (Planck 2015 TT+lowP)

① ***LSS redshift space distortions***: 6dFGS, SDSS, BOSS, WiggleZ
② ***LSS weak lensing***: CFHTLenS
③ ***X-ray/optical/SZ cluster counts***: CPPP, MaxBCG, ACT/SPT/Planck

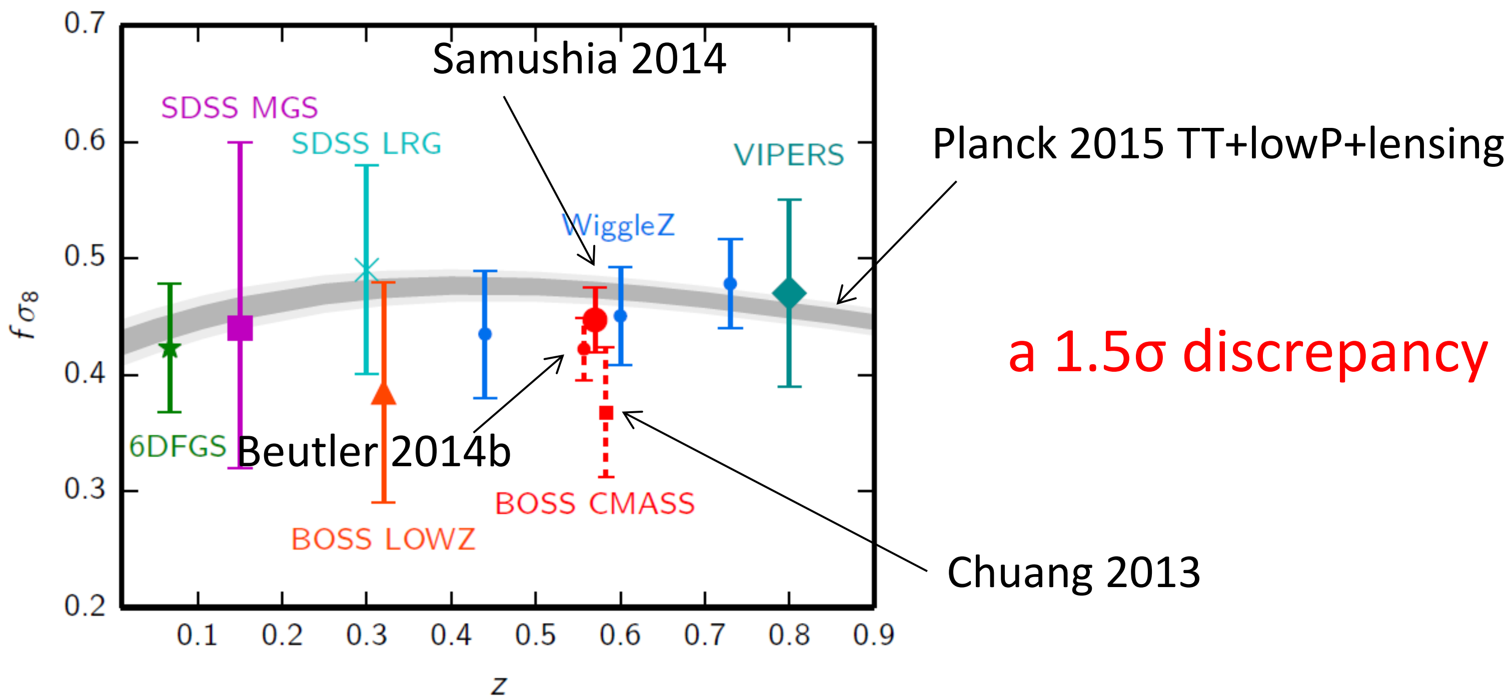

a 1.5σ discrepancy

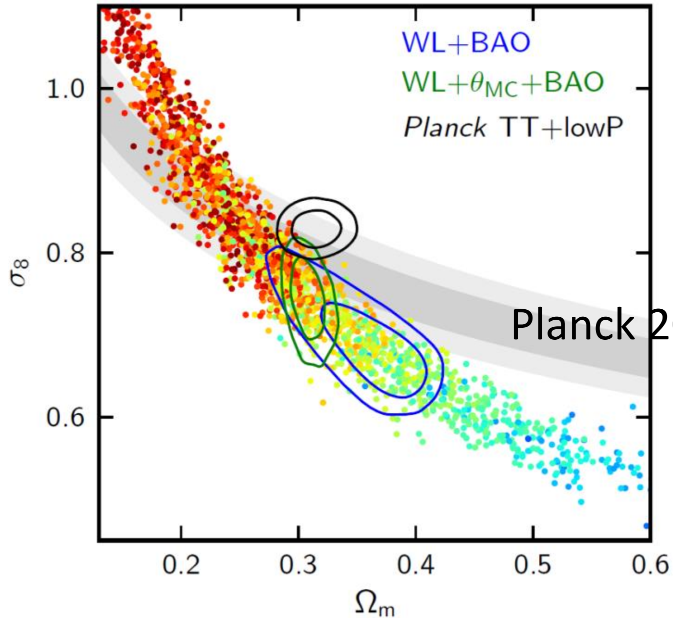

a strong discrepancy

Planck 2015 lensing

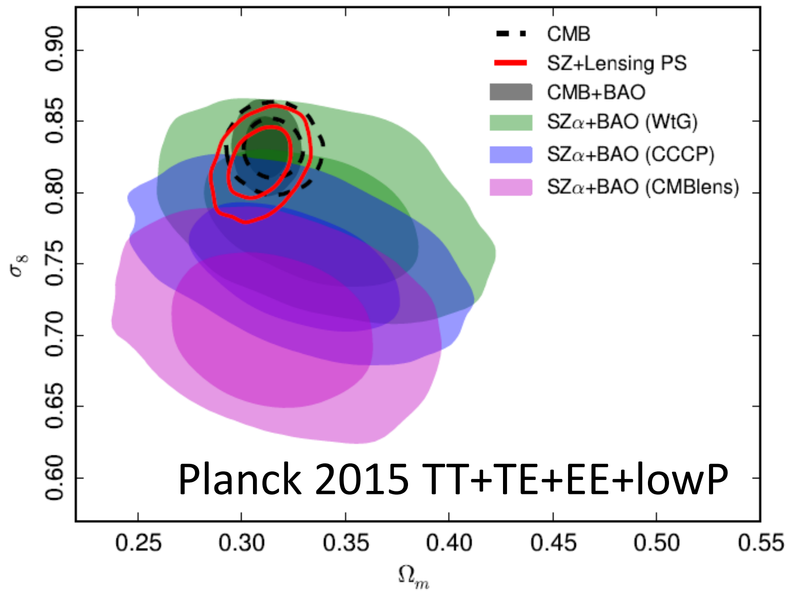

Prior name	Quantity	Value & Gaussian errors
Weighing the Giants (WtG)	$1-b$	0.688 ± 0.072
Canadian Cluster Comparison Project (CCCP)	$1-b$	0.780 ± 0.092
CMB lensing (LENS)	$1/(1-b)$	0.99 ± 0.19
Baseline 2013	$1-b$	$0.8\,[-0.1, +0.2]$

JW Hu, RG Cai, ZK Guo, B Hu, JCAP 05 (2014) 020.

6. 标准模型 — 原初曲率扰动的谱指标

$n_s = 0.9603 \pm 0.0073$ (Planck 2013 TT+WP)

$n_s = 0.9655 \pm 0.0062$ (Planck 2015 TT+lowP)

a 0.7σ shift

a 5.6σ deviation from the scale-invariance, i.e., dynamical

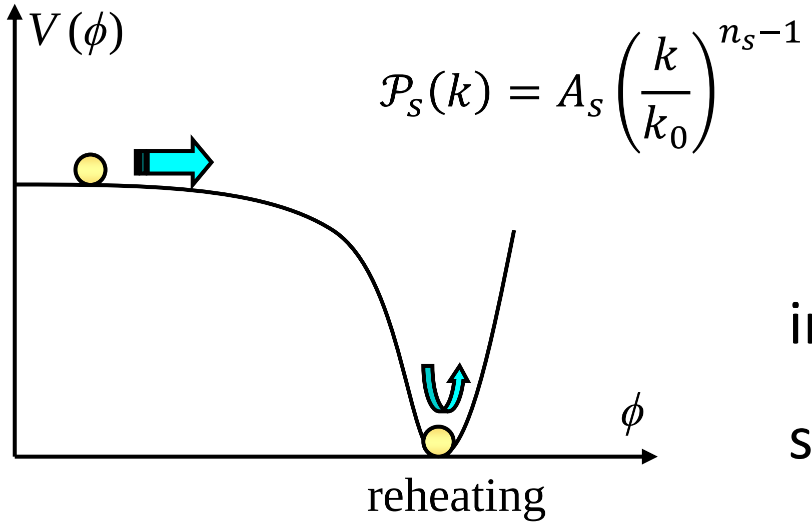

inflationary scenario

since 1981

评论：

- 普朗克研究组终于可以脱离其他天文观测数据，独立分析宇宙学参数。
- 也正是非常精确的数据使得分析结果与其他天文观测之间的不一致突显出来。
- 这些不一致性暗示了，要么观测数据有未考虑的系统误差，要么标准模型并不能很好地描述宇宙的演化规律。

7. 超标准模型 — 暗能量和修改引力

① ***Reliability of Type Ia SNe***：不相信 2011 Nobel Prize

② ***Cosmological principle***: 不自然 LTB

③ ***Dark energy***: 不理解

④ ***Modified gravity***: 不喜欢

$$w = -1.13^{+0.24}_{-0.14}$$ (95%, Planck 2013 TT+WP+BAO)

$$w = -1.54^{+0.62}_{-0.50}$$ (95%, Planck 2015 TT+lowP)

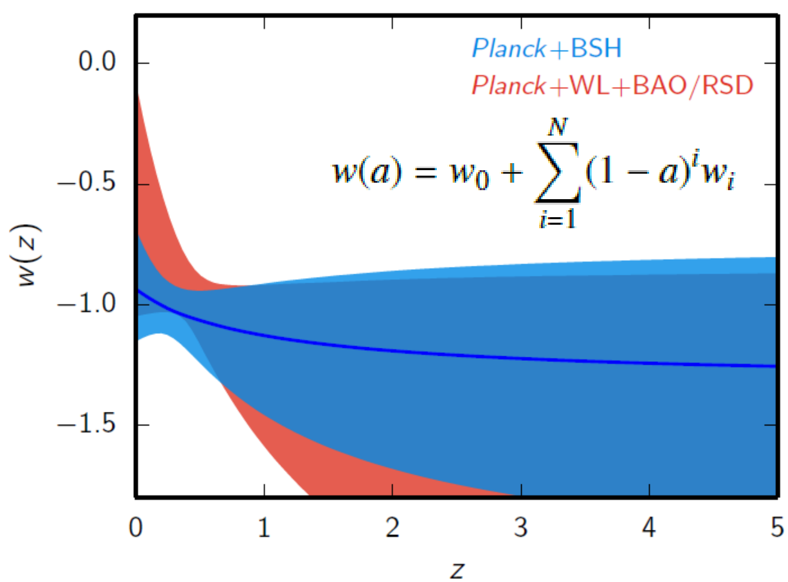

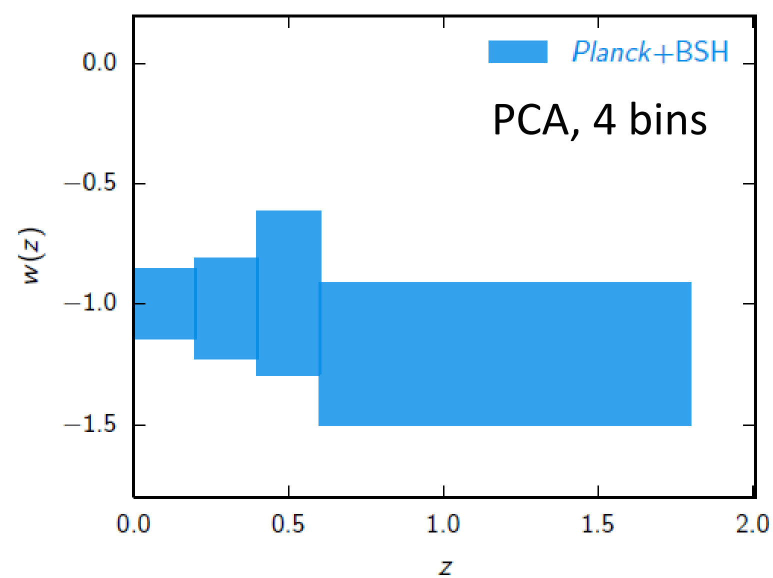

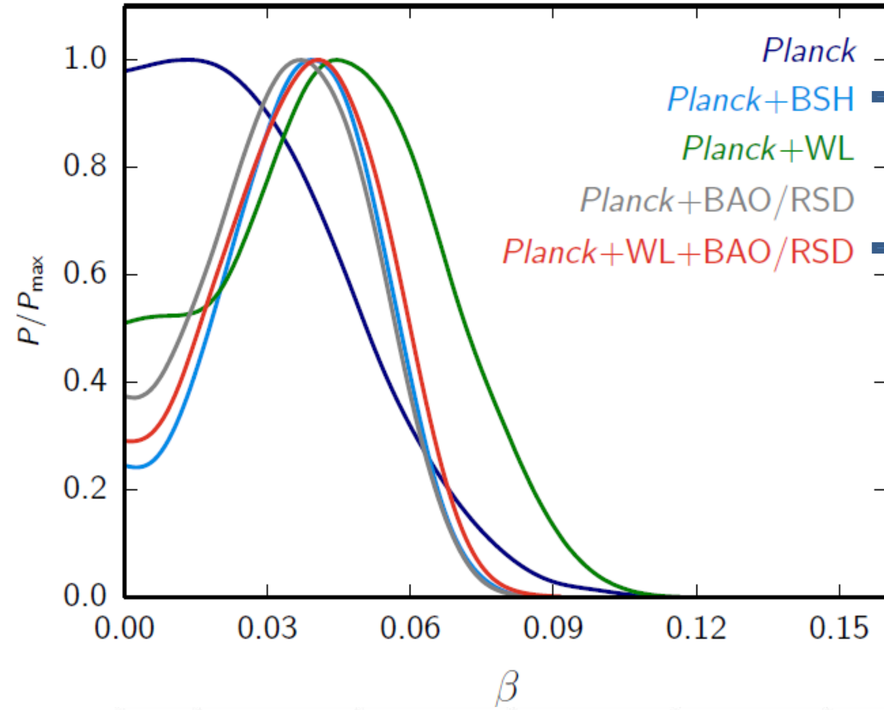

a 2.5σ deviation

a 2.3σ deviation

$$\rho'_\phi + 3\mathcal{H}\rho_\phi(1+w_\phi) = \beta\rho_c\phi'$$
$$\rho'_c + 3\mathcal{H}\rho_c = -\beta\rho_c\phi'$$
$$V(\phi) = \frac{V_0}{\phi^\alpha}$$

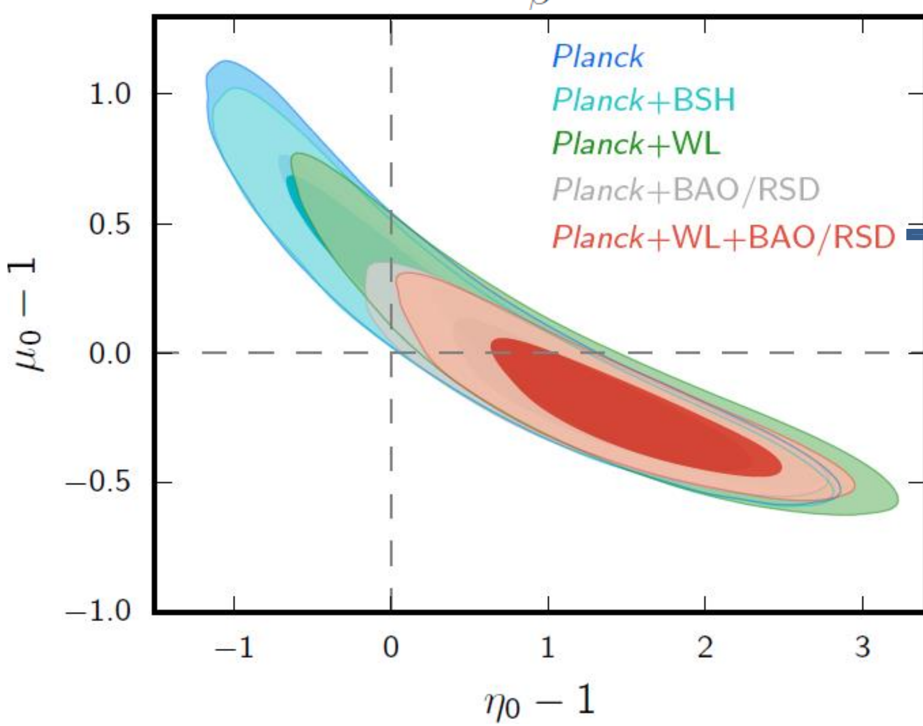

a 3σ departure

$$\eta(a,k) \equiv \frac{\Phi}{\Psi}$$
$$-k^2\Psi \equiv 4\pi G a^2 \mu(a,k)\rho\Delta$$

scale-independent &
dark-energy related

8. 超标准模型 — 原初引力波

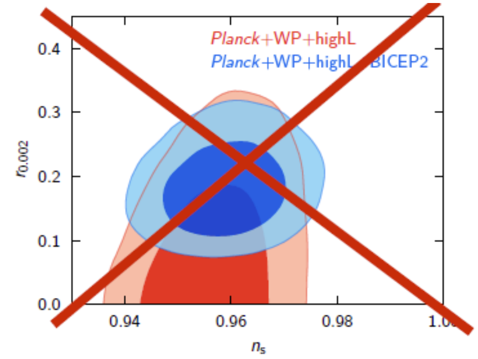

$$r_{0.002} < 0.12 \ \ (95\%, \text{Planck 2013 TT+WP})$$

$$r_{0.002} < 0.10 \ \ (95\%, \text{Planck 2015 TT+lowP})$$

$$r_{0.002} < 0.08 \ \ (95\%, \text{Planck 2015 TT+lowP+BKP})$$

Is the BB mode a smoking gun?

$$\text{sclar mode} \Longrightarrow TT, TE, EE; \quad \text{tensor mode} \Longrightarrow TT, TE, EE, BB$$

In slow-roll inflationary scenarios:

$$V^{1/4} \sim \left(\frac{r}{0.01}\right)^{1/4} 10^{16}\text{GeV}$$

Observable gravity waves imply inflation happened around the GUT scale.

$$\Delta\phi \sim \left(\frac{r}{0.002}\right)^{1/2} \left(\frac{N_*}{60}\right) M_{pl}$$

Observable gravity waves imply super-Planckian field excursion.

Selected for a Viewpoint in *Physics*
PRL **112,** 241101 (2014) PHYSICAL REVIEW LETTERS week ending 20 JUNE 2014 25P

Detection of *B*-Mode Polarization at Degree Angular Scales by BICEP2

P. A. R. Ade,[1] R. W. Aikin,[2] D. Barkats,[3] S. J. Benton,[4] C. A. Bischoff,[5] J. J. Bock,[2,6] J. A. Brevik,[2] I. Buder,[5] E. Bullock,[7] C. D. Dowell,[6] L. Duband,[8] J. P. Filippini,[2] S. Fliescher,[9] S. R. Golwala,[2] M. Halpern,[10] M. Hasselfield,[10] S. R. Hildebrandt,[2,6] G. C. Hilton,[11] V. V. Hristov,[2] K. D. Irwin,[12,13,11] K. S. Karkare,[5] J. P. Kaufman,[14] B. G. Keating,[14] S. A. Kernasovskiy,[12] J. M. Kovac,[5,*] C. L. Kuo,[12,13] E. M. Leitch,[15] M. Lueker,[2] P. Mason,[2] C. B. Netterfield,[4,16] H. T. Nguyen,[6] R. O'Brient,[6] R. W. Ogburn IV,[12,13] A. Orlando,[14] C. Pryke,[9,7,†] C. D. Reintsema,[11] S. Richter,[5] R. Schwarz,[9] C. D. Sheehy,[9,15] Z. K. Staniszewski,[2,6] R. V. Sudiwala,[1] G. P. Teply,[2] J. E. Tolan,[12] A. D. Turner,[6] A. G. Vieregg,[5,15] C. L. Wong,[5] and K. W. Yoon[12,13]

(BICEP2 Collaboration)

tensor-to-scalar ratio $r = 0.20^{+0.07}_{-0.05}$, with $r = 0$ disfavored at 7.0σ. Accounting for the contribution of foreground, dust will shift this value downward by an amount which will be better constrained with upcoming data sets.

DOI: 10.1103/PhysRevLett.112.241101 PACS numbers: 98.70.Vc, 04.80.Nn, 95.85.Bh, 98.80.Es

Selected for a Viewpoint in *Physics*
PRL **114,** 101301 (2015) PHYSICAL REVIEW LETTERS week ending 13 MARCH 2015 17P

Joint Analysis of BICEP2/*Keck Array* and *Planck* Data

P. A. R. Ade *et al.**
(BICEP2/Keck and Planck Collaborations)
(Received 21 January 2015; published 9 March 2015)

We report the results of a joint analysis of data from BICEP2/*Keck Array* and *Planck*. BICEP2 and *Keck Array* have observed the same approximately 400 deg^2 patch of sky centered on RA 0 h, Dec. −57.5°. The combined maps reach a depth of 57 nK deg in Stokes Q and U in a band centered at 150 GHz. *Planck* has observed the full sky in polarization at seven frequencies from 30 to 353 GHz, but much less deeply in any given region (1.2 μK deg in Q and U at 143 GHz). We detect 150×353 cross-correlation in B modes at high significance. We fit the single- and cross-frequency power spectra at frequencies ≥ 150 GHz to a lensed-ΛCDM model that includes dust and a possible contribution from inflationary gravitational waves (as parametrized by the tensor-to-scalar ratio r), using a prior on the frequency spectral behavior of polarized dust emission from previous *Planck* analysis of other regions of the sky. We find strong evidence for dust and no statistically significant evidence for tensor modes. We probe various model variations and extensions, including adding a synchrotron component in combination with lower frequency data, and find that these make little difference to the r constraint. Finally, we present an alternative analysis which is similar to a map-based cleaning of the dust contribution, and show that this gives similar constraints. The final result is expressed as a likelihood curve for r, and yields an upper limit $r_{0.05} < 0.12$ at 95% confidence. Marginalizing over dust and r, lensing B modes are detected at 7.0σ significance.

DOI: 10.1103/PhysRevLett.114.101301 PACS numbers: 98.70.Vc, 04.80.Nn, 95.85.Bh, 98.80.Es

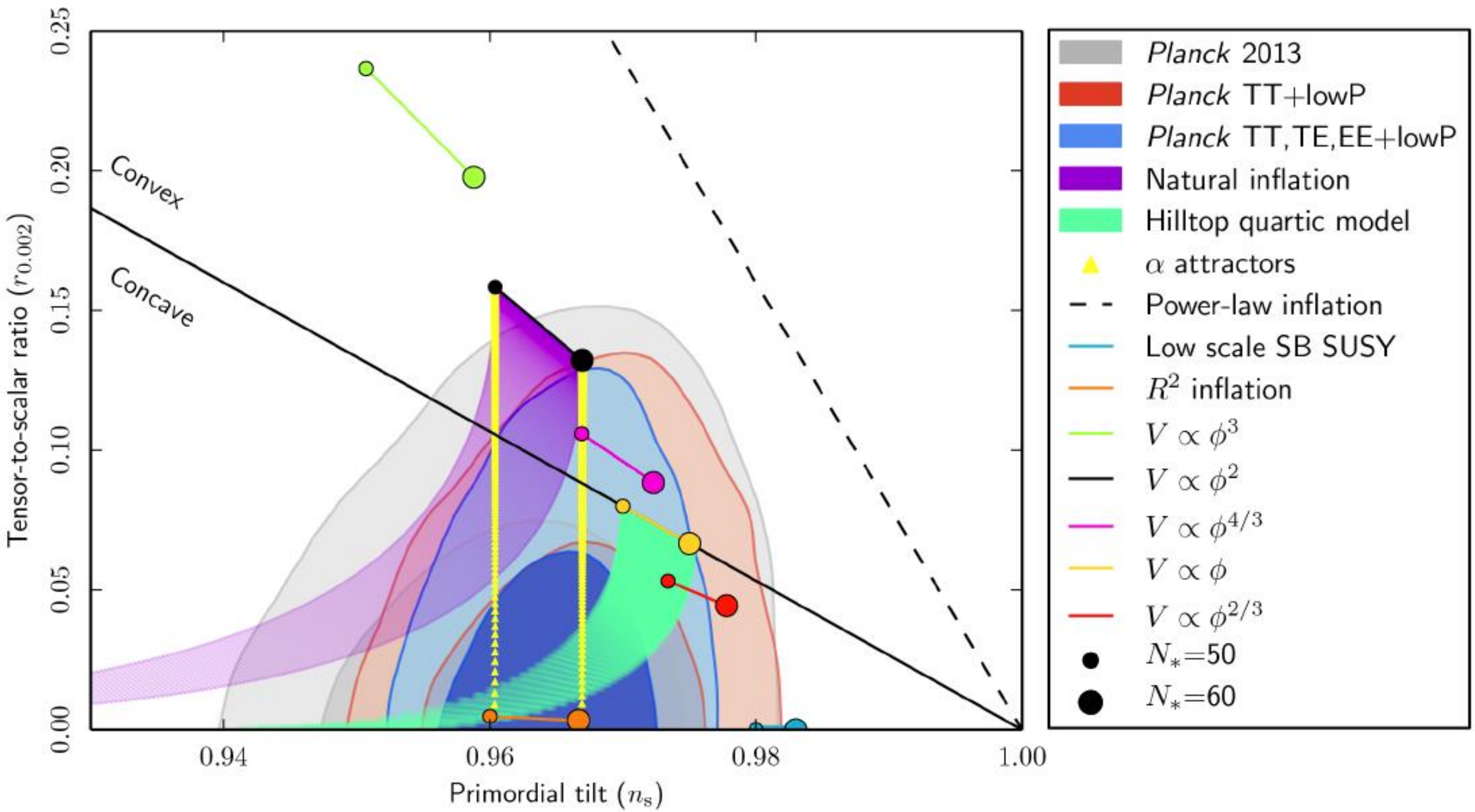

$$V(\phi) = \Lambda^4 \left(1 - \frac{\phi^p}{\mu^p}\right) \text{ (Hilltop)} \qquad V(\phi) = \Lambda^4 \left[1 + \cos\left(\frac{\phi}{f}\right)\right] \text{ (Natural)}$$

$$V(\phi) = \Lambda^4 \left(1 - e^{-\sqrt{2}\phi/(\sqrt{3\alpha}M_{pl})}\right)^2 \text{ (α attractors, } R^2\text{/nonminimal for α = 1)}$$

ZK Guo, N. Ohta, S. Tsujikawa, Phys. Rev. D75 (2007) 023520; ZK Guo, D.J. Schwarz, Phys. Rev. D80 (2009) 063523;
ZK Guo, D.J. Schwarz, Phys. Rev. D81 (2010) 123520; PX Jiang, JW Hu, ZK Guo, Phys. Rev. D88 (2013) 123508.

$$K = -3\ln\left(1 + \frac{\Phi + \bar{\Phi} + (\Phi + \bar{\Phi})^4}{\sqrt{3}}\right), \qquad W = m\left(\Phi^3 + a e^{i\theta}\Phi + b\right)$$

$$V(\chi) = m^2\left(\frac{9}{4}\chi^4 - \sqrt{6}a\sin\theta\,\chi^3 + 3\left(\sqrt{3}b - a\cos\theta\right)\chi^2 + a^2 - 2\sqrt{3}ab\cos\theta\right)$$

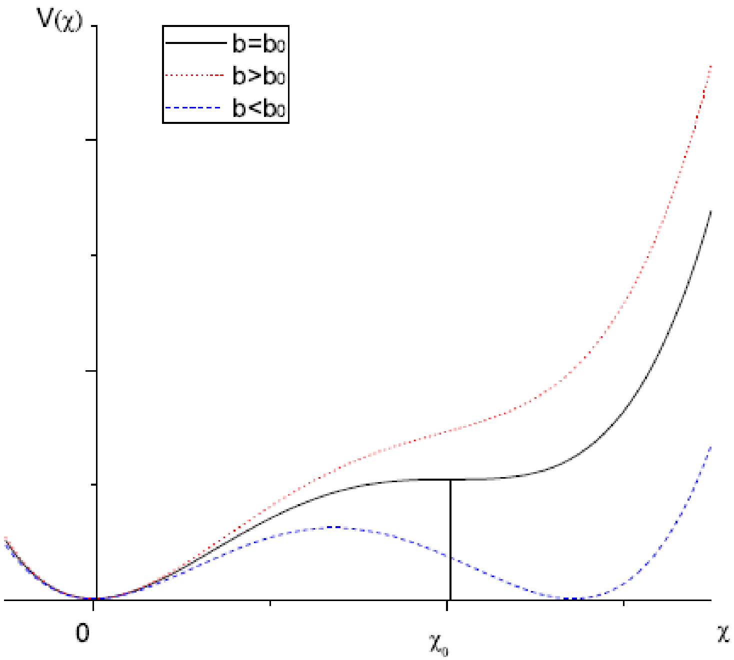

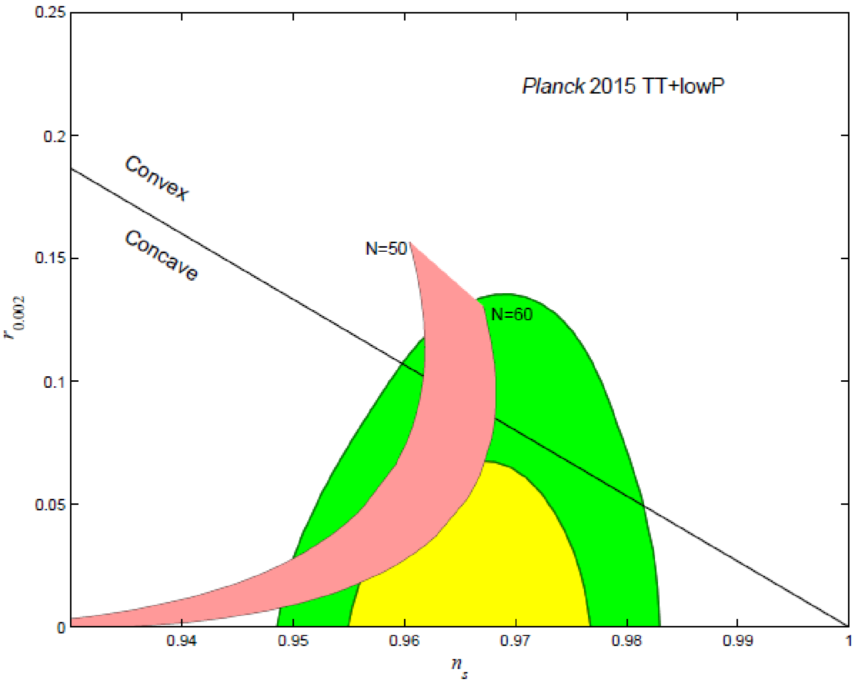

TJ Gao, ZK Guo, arXiv:1503.05643.

9. 超标准模型 — 原初曲率扰动的功率谱性质

$$\frac{dn_s}{d\ln k} = -0.013 \pm 0.009 \quad \text{(Planck 2013 TT+WP)}$$

$$\frac{dn_s}{d\ln k} = -0.0084 \pm 0.0082 \quad \text{(Planck 2015 TT+lowP)}$$

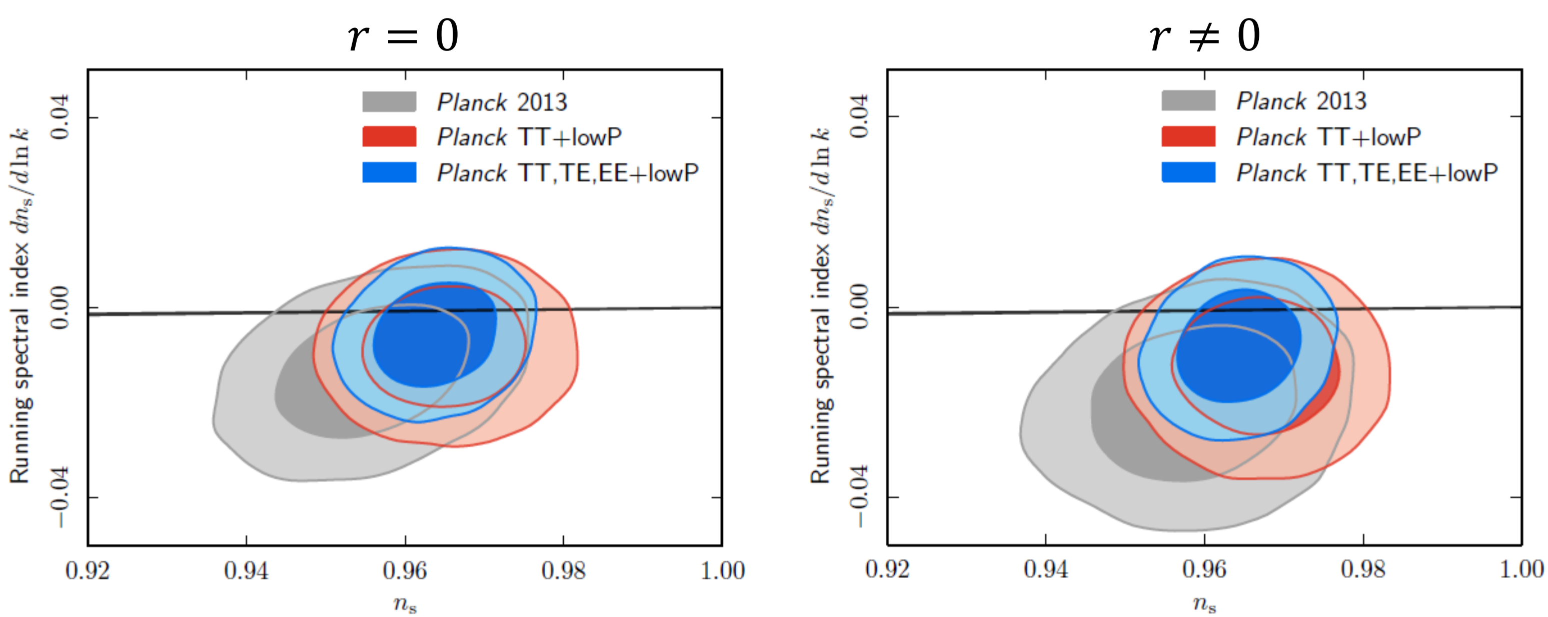

ZG Liu, ZK Guo, YS Piao, Phys. Rev. D88 (2013) 063539; ZG Liu, ZK Guo, YS Piao, EPJC 74 (2014) 3006.

Simple parameterizations of the power spectrum: power-law with exponential cut-off, broken power-law, step-like, logarithmic oscillations, linear oscillations

Reconstruction of the potential:

Reconstruction of the power spectrum:

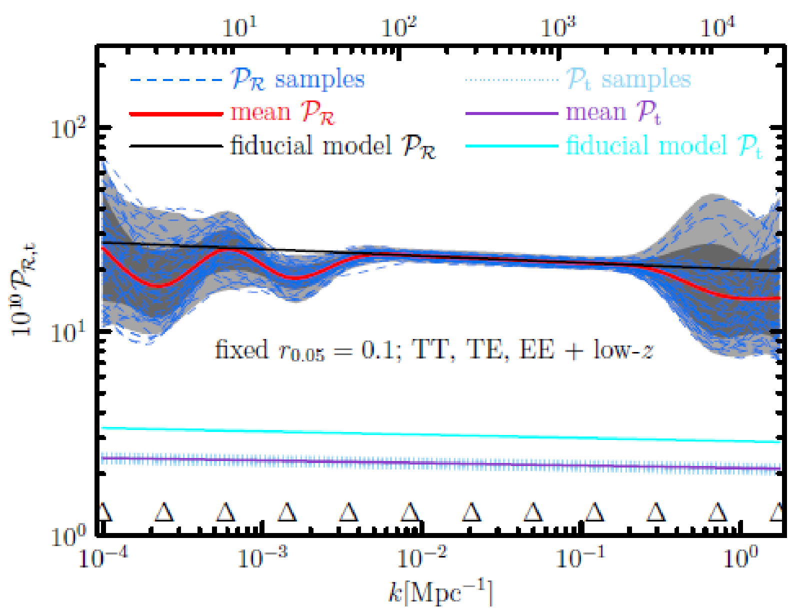

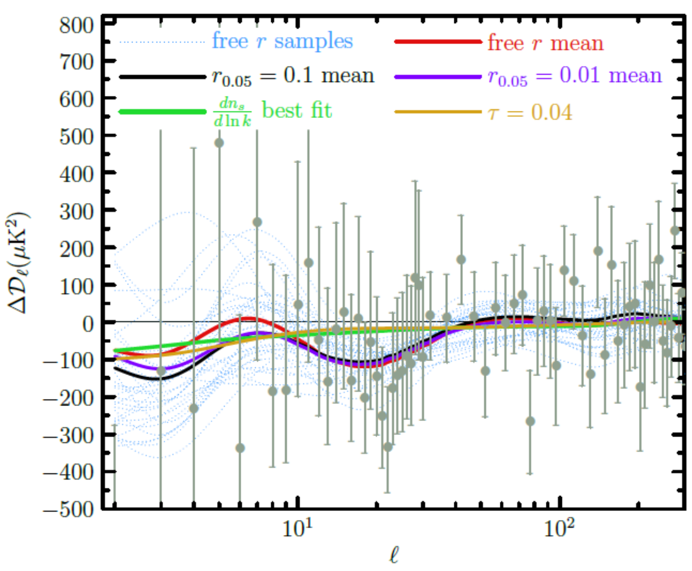

a dip at $k \sim 0.002\ \mathrm{Mpc}^{-1}$, around $l \sim 20-30$

ZK Guo, D J. Schwarz, YZ Zhang, JCAP 08 (2011) 031; ZK Guo, YZ Zhang, JCAP 11 (2011) 032; ZK Guo, YZ Zhang, Phys. Rev. D85 (2012) 103519; B Hu, JW Hu, ZK Guo, RG Cai, Phys. Rev. D90 (2014) 023544 .

10. 超标准模型 — 同曲率扰动

Initial conditions: CDI, NDI, NVI

Additional degrees of freedom during inflation: axion, curvaton

Parameterization: $\{\mathcal{P}_{\mathcal{RR}}, n_{\mathcal{RR}}, \mathcal{P}_{\mathcal{JJ}}, n_{\mathcal{JJ}}, \mathcal{P}_{\mathcal{RJ}}, n_{\mathcal{RJ}}\}$

$$\cos\Delta(k) = \frac{\mathcal{P}_{\mathcal{RJ}}}{\sqrt{\mathcal{P}_{\mathcal{RR}}\mathcal{P}_{\mathcal{JJ}}}}, \qquad \beta_{iso}(k) = \frac{\mathcal{P}_{\mathcal{JJ}}}{\mathcal{P}_{\mathcal{RR}} + \mathcal{P}_{\mathcal{JJ}}}$$

If Δ is scale-independent, $n_{\mathcal{RJ}} = \frac{1}{2}(n_{\mathcal{RR}} + n_{\mathcal{JJ}})$

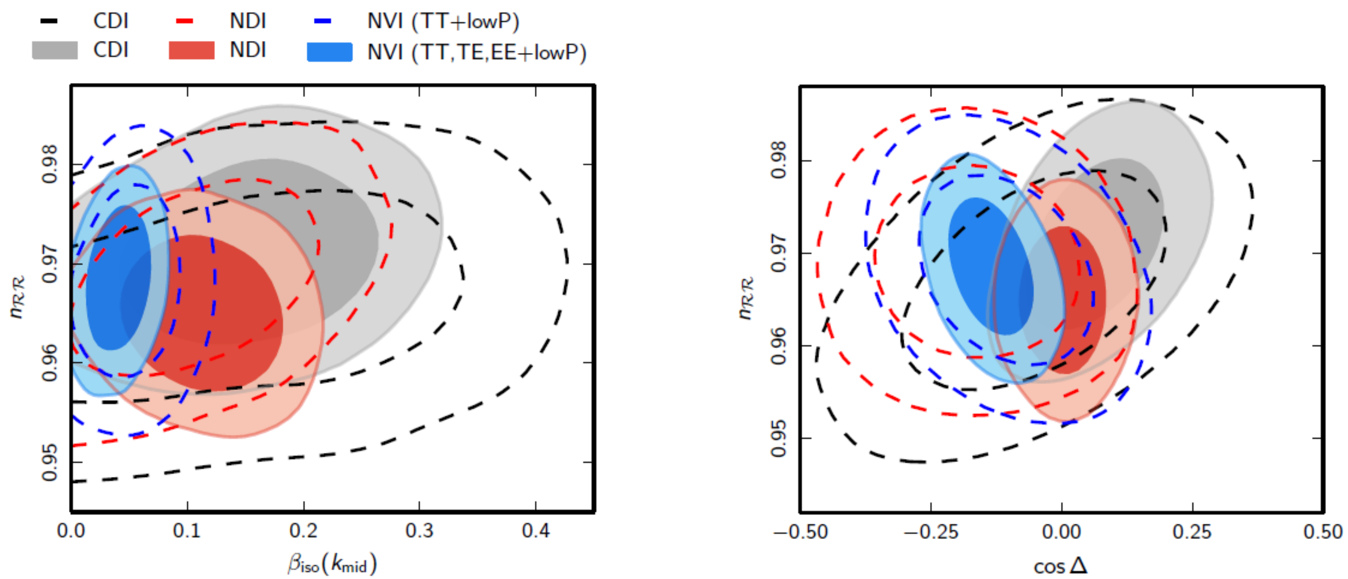

Uncorrelated axion CDI: $\mathcal{P}_{\mathcal{R}\mathcal{I}} = 0, n_{\mathcal{I}\mathcal{I}} = 1$

Fully correlated curvaton CDI: $\cos\Delta = 1, n_{\mathcal{I}\mathcal{I}} = n_{\mathcal{R}\mathcal{R}} = n_{\mathcal{R}\mathcal{I}}$

Fully anticorrelated curvaton CDI: $\cos\Delta = -1, n_{\mathcal{I}\mathcal{I}} = n_{\mathcal{R}\mathcal{R}} = n_{\mathcal{R}\mathcal{I}}$

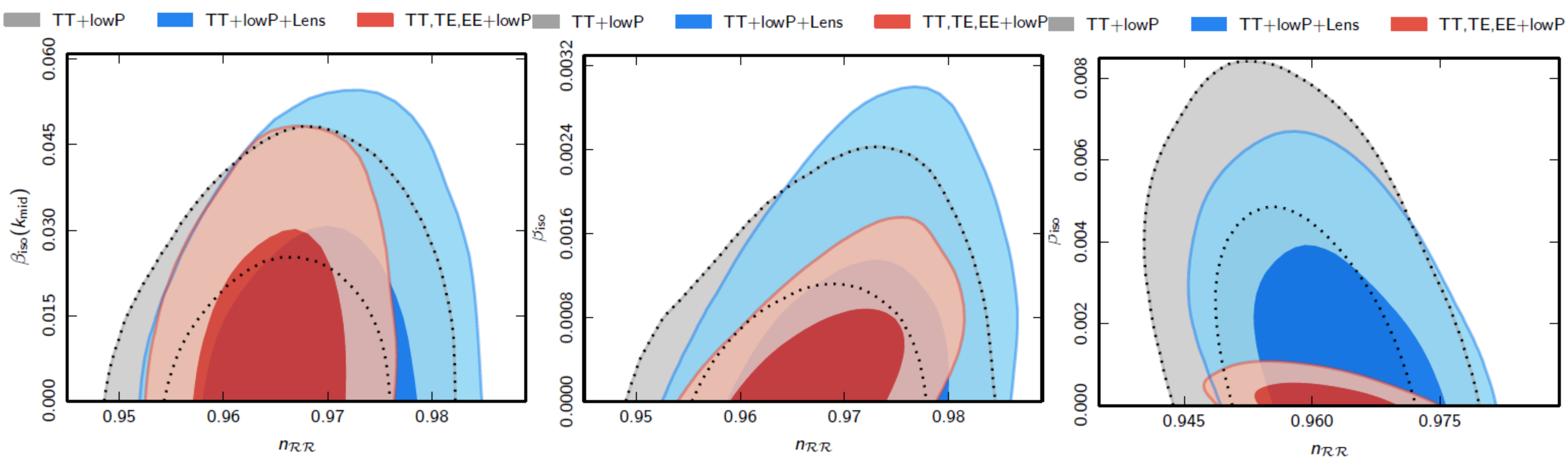

11. 超标准模型 — 原初非高斯

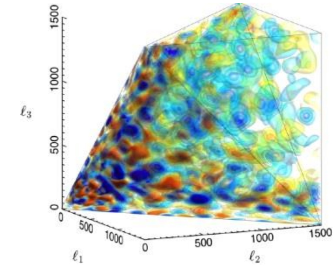

$f_{NL}^{local} = 2.7 \pm 5.8,\ f_{NL}^{equil} = -42 \pm 75,\ f_{NL}^{ortho} = -25 \pm 39$ (Planck 2013 T)

$f_{NL}^{local} = 0.8 \pm 5.0,\ f_{NL}^{equil} = -4 \pm 43,\ f_{NL}^{ortho} = -26 \pm 21$ (Planck 2015 T+E)

Optimal bispectrum estimators: KSW, binned, modal

Foreground-cleaned maps: SMICA, SEVEM, NILC, Commander

One of the most powerful tests of inflation:

- ✓ models with a non-standard kinetic term

$$B_\Phi^{equil}(k_1,k_2,k_3) = 6A^2 f_{NL}^{equil}\left\{-\left[\frac{1}{k_1^{4-n_s}k_2^{4-n_s}} + 2\text{ perm.}\right] - \frac{2}{(k_1k_2k_3)^{2(4-n_s)/3}} + \left[\frac{1}{k_1^{(4-n_s)/3}k_2^{2(4-n_s)/3}k_3^{4-n_s}} + 5\text{perm.}\right]\right\}$$

$$B_\Phi^{ortho}(k_1,k_2,k_3) = 6A^2 f_{NL}^{ortho}\left\{-\left[\frac{3}{k_1^{4-n_s}k_2^{4-n_s}} + 2\text{ perm.}\right] - \frac{8}{(k_1k_2k_3)^{2(4-n_s)/3}} + \left[\frac{3}{k_1^{(4-n_s)/3}k_2^{2(4-n_s)/3}k_3^{4-n_s}} + 5\text{perm.}\right]\right\}$$

- ✓ multiple-field models $B_\Phi^{local}(k_1,k_2,k_3) = 2f_{NL}^{local}[P_\Phi(k_1)P_\Phi(k_2) + 2\text{ perm.}]$

LF Li, RG Cai, ZK Guo, B Hu, Phys. Rev. D86 (2012) 044020 .

12. 超标准模型 — 空间拓扑

$$\Omega_k = -0.042^{+0.043}_{-0.048}$$ (95%, Planck 2013 TT+WP+highL)

$$\Omega_k = -0.052^{+0.049}_{-0.055}$$ (95%, Planck 2015 TT+lowP)

Simple topology: R^3, S^3, H^3

S^3 at 2σ CL

$$\Omega_k(t) \equiv -\frac{k}{a^2H^2} \rightarrow 0 \text{ (inflation)}$$

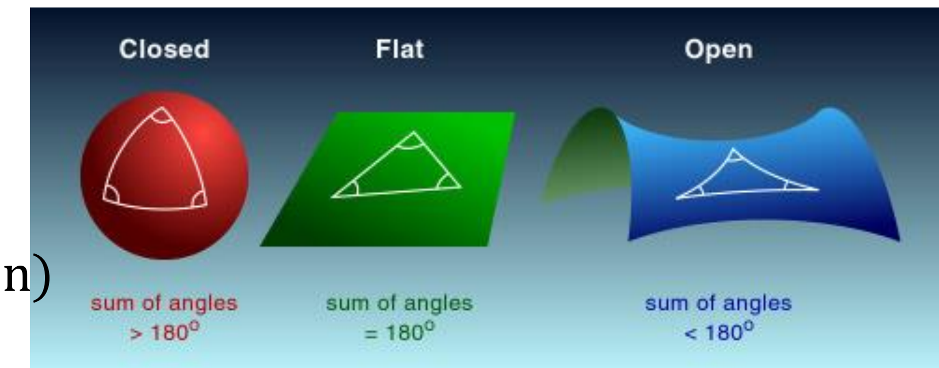

Non-trivial topology: T^3

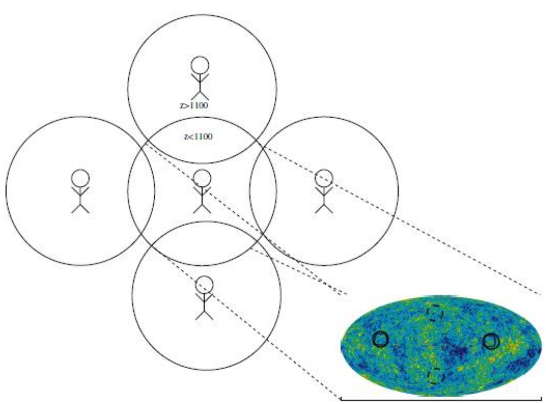

The size of the fundamental domain
$\mathcal{R}_i \geq 0.97\chi_{rec}$ at 99% CL

13. 超标准模型 — 中微子物理

$\sum m_\nu < 0.23\ \text{eV}$ (95%, Planck 2013 TT+WP+highL+BAO)

$\sum m_\nu < 0.21\ \text{eV}$ (95%, Planck 2015 TT+lowP+BAO)

Impact on CMB: early ISW effect, free streaming

Dark radiation: $N_{\text{eff}} = 3.046$ and $\sum m_\nu = 0.06\ \text{eV}$ in SM

$$\rho_\nu = N_{\text{eff}} \frac{7}{8} \left(\frac{4}{11}\right)^{4/3} \rho_\gamma$$

$N_{\text{eff}} = 3.30^{+0.54}_{-0.51}$ (95%, Planck 2013 TT+WP+highL+BAO)

$N_{\text{eff}} = 3.15 \pm 0.46$ (95%, Planck 2015 TT+lowP+BAO)

$N_{eff} > 0$ at 10 to 17σ CL

ZK Guo, QG Huang, RG Cai, YZ Zhang, Phys. Rev. D86 (2012) 065004 .

14. 超标准模型 — 原初氦合成

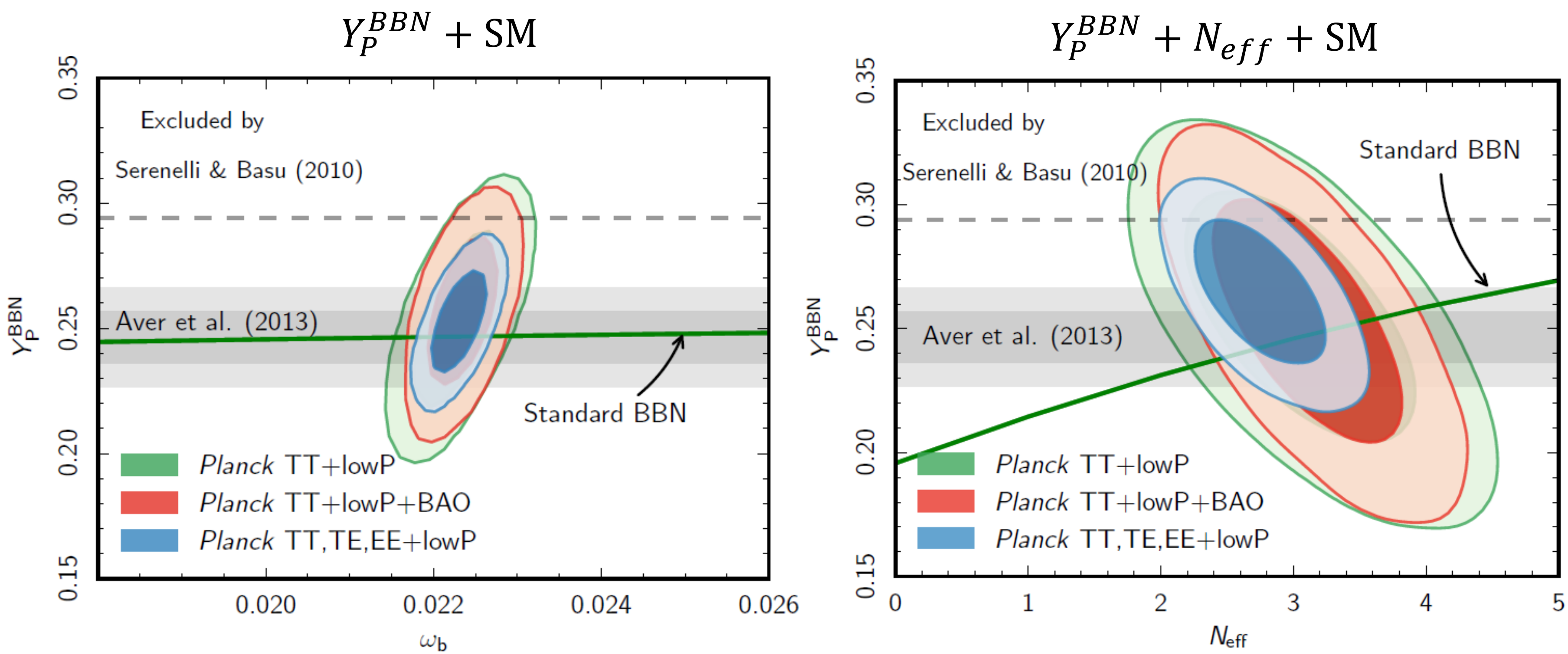

BBN prediction of the helium fraction: ω_b, N_{eff}

Aver 2013 observational bounds: $Y_P^{BBN} = 0.2465 \pm 0.0097$

Constraints from the Planck data:

ZK Guo, JW Hu, Phys. Rev. D87 (2013) 123519 .

15. 超标准模型 — 暗物质湮灭

$$\frac{dE}{dtdV}(z) = 2g\rho_{crit}^2 c^2 \Omega_c^2 (1+z)^6 p_{ann}(z), \qquad p_{ann}(z) \equiv f(z)\frac{\langle\sigma v\rangle}{m_\chi}$$

Effects on CMB: heating, ionizations, lyα excitations of the medium

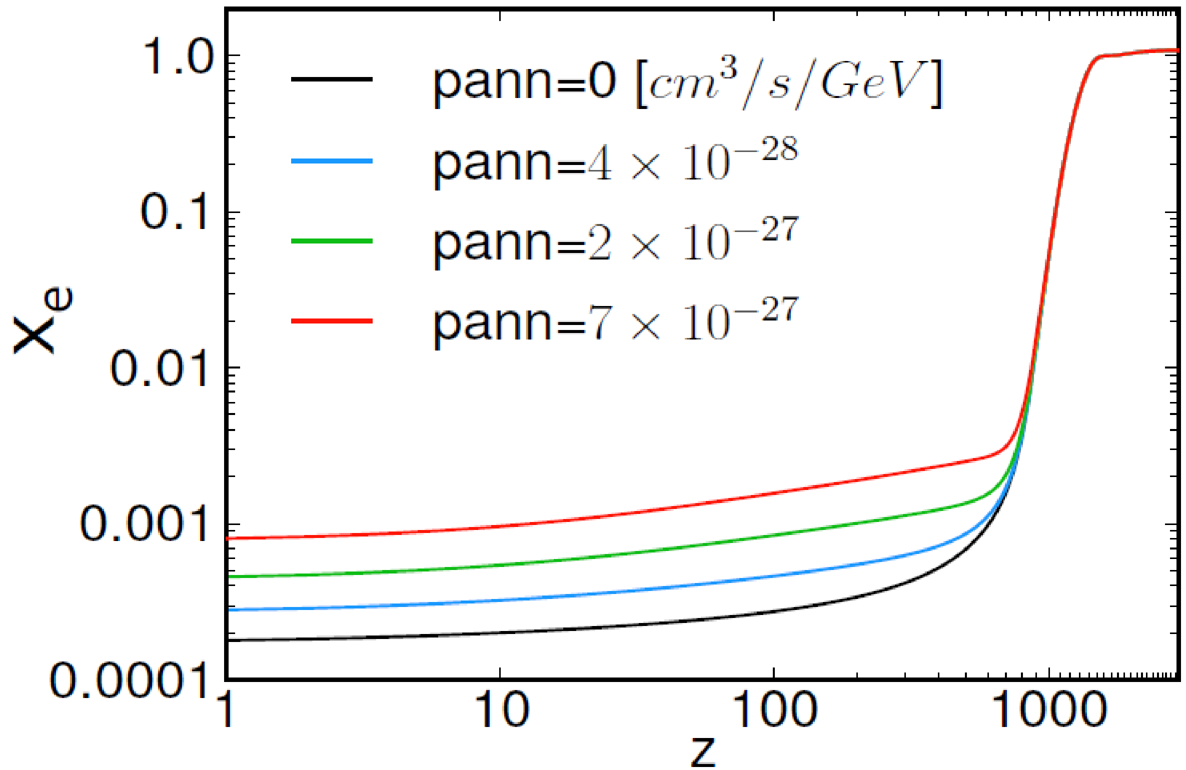

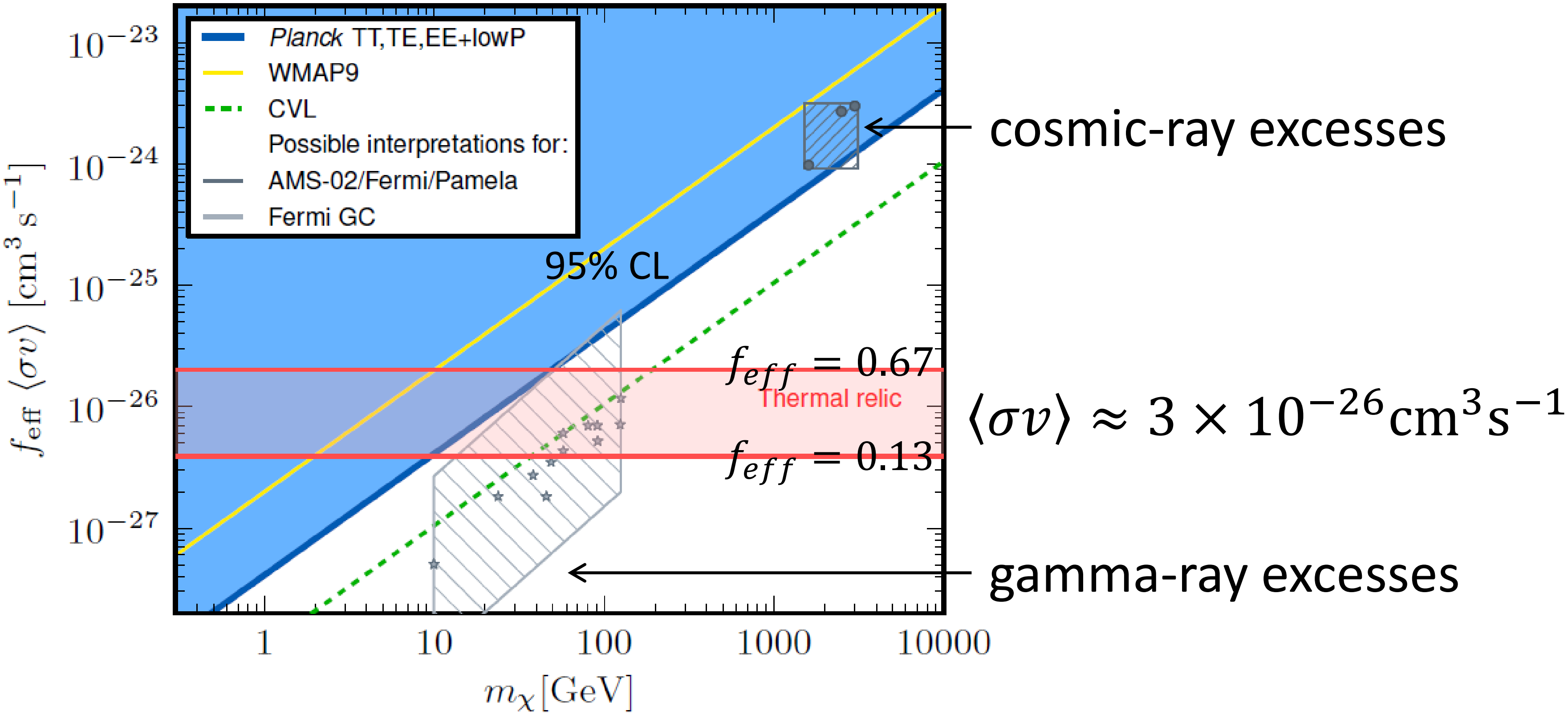

The Planck exclude at 95% CL a thermal relic cross-section for

$$\chi\bar{\chi} \rightarrow e^+e^-, f_{eff} \approx 0.6, m_\chi \leq 44 \text{ GeV}$$
$$\chi\bar{\chi} \rightarrow \mu^+\mu^-, f_{eff} \approx 0.2, m_\chi \leq 16 \text{ GeV}$$
$$\chi\bar{\chi} \rightarrow \tau^+\tau^-, f_{eff} \approx 0.15, m_\chi \leq 11 \text{ GeV}$$

16. 超标准模型 — 原初磁场

$B_{1Mpc} < 4.1\ \mathrm{nG}$ (95%, Planck 2013 TT+WP)

$B_{1Mpc} < 4.4\ \mathrm{nG}$ (95%, Planck 2015 TT+lowP)

Observations: $B \sim 1\ \mathrm{nG}$ in galaxies and galaxy clusters
Magnetogenesis: strong coupling, backreaction, perturbations
Effects of PMF on CMB:

① The energy momentum tensor of PMF source scalar, vector and tensor perturbations.
② PMF induce a Lorentz force on baryons modifying their evolution.

谢谢大家！